Heatlines Analysis of Natural Convection in an Enclosure Divided by a Sinusoidal Porous Layer and Filled by Cu-Water Nanofluid with Magnetic Field Effect

Hamzah, Hameed K.
Mechanical Engineering Department, College of Engineering, University of Babylon, Babylon, IRAQ

Kareem, Doaa F.
Power Mechanics Techniques Engineering Department, Al-Musaib Technical College, Babylon IRAQ

Ahmed, Saba Y.; Ali, Farroq H.
Mechanical Engineering Department, College of Engineering, University of Babylon, Babylon, IRAQ

Hatami, Mohammad*+
Department of Mechanical Engineering, Ferdowsi University of Mashhad, Mashhad, I.R. IRAN

ABSTRACT: *A numerical study is executed to analyze the steady-state heatlines visualization, fluid flow, and heat transfer inside a square enclosure with the presence of the magnetic field. The enclosure is divided into three layers, the right and left layers are filled with (Cu-Water) nanofluid while the center layer is sinusoidal porous and filled with the same nanofluid. Constant hot and cold temperature is applied to the right and left walls, respectively, the top and bottom walls are adiabatic. Galerkin finite element approach based on weak formulation is applied to solve the governing equations. The parameters studied are the number of undulation (N=1, 2 and 3), Rayleigh number ($10^3 \le Ra \le 10^6$), Darcy number ($10^{-5} \le Da \le 10^{-1}$), Hartmann number ($0 \le Ha \le 100$) and volume fraction ($0 \le \varphi \le 0.06$). Three cases were provided depending on the number of undulations of the porous medium layer. The results obtained that the absolute value of the maximum stream function decreases with the increase of the Hartmann number and the decrease of the Darcy number for all three cases of the wavy porous layer. Heatlines and isothermal lines increase as the Darcy number is increased. The average Nusselt number grows by increasing the Rayleigh number and decreasing the Hartmann number. The enhancement of heat transfer occurred for case (2) as the Darcy number increased at a constant $Ra=10^5$, Ha=40. Also, It can be concluded that there was an excellent agreement between this study and those of Hamida and Charrada, by an approximately maximum absolute error of 2.062%.*

KEYWORDS: *Nanofluid; Porous medium; Heatlines; Natural Convection; Sinusoidal Layer; Hartmann number.*

** To whom correspondence should be addressed.*
+ E-mail: m.hatami@xjtu.edu.cn & m-hatami@um.ac.ir
Other address : Al-Awsat Technical University, Al-Furat, Kufa, IRAQ
1021-9986/2022/6/2046-2070 25/$/7.05

INTRODUCTION

Applications of natural convection heat transfer within a cavity partially filled with porous and nanofluid layers appeared in the past few decades for many engineering applications such as solar energy, cooling of nuclear reactors and electronic systems, heating and cooling buildings, lubrication of components, and packed bed reactor,…etc (*Al-Zamily*, 2015 [1]).

Many researchers have studied the influences of magnetic field on the heat transfer characteristics and fluid flow under natural convection in enclosures filled with different types of nano-fluids due to its importance in many engineering applications such as geothermal energy extractions, the growth of the crystal in fluids, the casting of metal, and the fusion nuclear reactors. The effects of nano-particles volume fraction and Rayleigh number on the rate of natural convection heat transfer inside a square enclosure filled with different types of nanofluid (Cu-water or Al_2O_3-water) were studied numerically by (*Ghahremani*, 2018 [2], *Boulahia, et al.*, 2016[3], *Jmai et al.*, 2013 [4], *Khanafer, et al.*, 2003 [5]). It's found that the rate of heat transfer was enhanced by increasing the volume fraction of nanoparticles at any given value of the Rayleigh number.

The reason for using the nanoparticles can be attributed to it's high thermal conductivity and higher stability compared with conventional liquids. Employed the double multiple-relaxation-time (MRT) thermal lattice Boltzmann method to study numerically the heat transfer and magneto-hydrodynamic (MHD) flow in an inclined square cavity filled with nanofluid (Cu-water), with 4 heat sources in (*Zhang, et al.*, 2016 [6]) which analyzed the effects of the dimensionless parameters such as Rayleigh number, Hartmann number, the volume fraction of nanoparticles, and inclination angle on fluid flow as well as heat transfer. It was concluded that the Hartmann number and angle of inclination possess a significant impact on the flow field and patterns of temperature. Also, it's found that at any value of Rayleigh number the average Nusselt number increases by increasing the volume fraction of nanoparticles. (*Santra*, 2008 [7]), investigated the heat transfer enhancement of a non-Newtonian nanofluid in a partially heated square enclosure filled by copper nanoparticles (0.05%-5% vol.) with the Rayleigh number range (10^4-10^7). The Ostwald-deWaeles model is used to calculate the shear stresses. It was observed that the heat transfer reduced when the nanoparticles concentration arises.

While the papers that deal with the enhancement of heat transfer by porous media in an enclosure have been great attention. There are two reasons for utilizing porous media in industrial applications. Firstly, the dissipation region is larger than the traditional fins that promote heat transfer. Secondly, the irregular movement of the fluid flow about the individual beads blends the fluids more effectively. (*Muthtamilselvan, et al.*, 2018 [8]), numerically studied the unsteady natural convective transfer in a lid-driven porous enclosure has the shape square filled with nano-fluid (Cu-water). The effect of different lengths and various locations of heat sources on the enhancement of heat transfer was investigated. The length of the heater equals 1/3 of the heat source and locations of the heat source at the top of the hot wall yield the best enhancement in heat transfer. (*Alsabery, et al.*, 2017 [9]), employed numerically by finite volume method the natural convective heat transfer in a square inclined cavity consisting of two layers (nano-layer and porous layer). The temperature of the vertical walls varies with time in a Sinusoidal form. The results showed that the increment of the porous layer significantly affects the rate of heat transfer. Furthermore, the addition of nano-particles leads to enhance natural convective transfer. (*Ismael, et al.*, 2016 [10]), studied numerically the steady conjugate free convection–conduction transfer and entropy generation in a square porous enclosure that is packed with (CuO–water) nano-fluids and was partially heated by a solid wall have the form isosceles triangle occupying the lower left corner. It's observed that, at the lower value of Rayleigh number, the rates of heat transfer and entropy generation increase with the growth in thickness of the solid wall. Additionally, The results mentioned that adding nano-particles into pure water improves the overall heat transfer and increases entropy generation, especially at a lower value of Rayleigh numbers. (*Alsabery, et al.*, 2016 [11]), solved the problem of conjugate natural convection inside a cavity having the shape square is filled with different nano-fluid particles with sinusoidal temperature variations on both horizontal walls. The results showed that the heat transfer rate was significantly improved by incrementing the thickness of the solid wall. (*Badruddin, et al.*, 2015 [12]), investigated numerically the conjugate natural convection

transfer across an annulus porous medium confined among two-finite thickness solid walls that existed at the inner and outer radius of the annulus. It was found that when the thickness of the wall is smaller, there is no significant change in the temperature inside the inner solid wall. The differentially heated enclosure was widely used to emulate free convection transfer inside systems utilizing nano-fluids and/or porous media.

(*Alsabery,et al.,*2015 [13]), analyzed numerically the natural convective transfer through the heatlines, streamlines, and isotherms across an inclined trapezoidal enclosure that is partially packed with porous nano-fluid and partially filled with nano-Newtonian fluid. It was found that adding nano-particles into the base fluid (water) enhanced the rate of heat transfer and the convection was influenced by the inclination angle of the enclosure. (*Selimefendigil* and *Öztop*, 2014 [14]), examined numerically the natural convection and entropy generation in a square enclosure that is packed with nanofluids under the influence of a magnetic field. It was found that as the Hartmann number increases, the average heat transfer decrease. (*Al-Farhany* and *Turan*, 2011 [15]), in a square enclosure confined between two-finite thickness walls at the top and the bottom of the enclosure. The enclosure is filled with a fluid-saturated porous medium, and they concluded that as the thermal conductivity ratio increases the average Nusselt number increases. (*Aminossadati* and *Ghasemi*, 2009 [16]), investigated free convection cooling of a heat source placed on the bottom wall of an enclosure that is packed with different types of nano-fluids. The top and vertical partitions of the enclosure had been maintained at a relatively low temperature. The results proved that the type of nano-particles and the position and length of the heat source greatly affect the heat source's maximum temperature. Also, it was found that adding nano-particles into the base fluid (water) enhances its cooling performance, especially at lower values of Rayleigh numbers. (*Abu-Nada* and *Oztop*, 2009 [17]) considered different inclination angles (0-120º) and Rayleigh numbers (10^3-10^5) to study the effect of Cu-water nanofluid natural convection in a square enclosure (*Ammar et al.*, 2019 [28]). The results revealed that heat transfer improvements occurred when the nanoparticles' volume fraction increased at low Rayleigh numbers.

Differentially heated and vertically partially layered porous enclosures filled with a different nanofluid have been studied experimentally or numerically by different researchers to find the natural convection heat transfer behavior, such as:

(*Hussain and Rahomey*, 2018 [18]) study the natural convection inside a square enclosure due to the temperature difference between a hot inner cylinder with various shapes (circular, triangular, elliptic, rectangular, and rhombic) and a cold outer wall. The enclosure is occupied with Ag-Water nanofluid superposed porous nanofluid. The effect of horizontally wavy nanofluid (Cu-water)/ porous interface on the natural convection of a nanofluid in an enclosure with a partially layered the non-Darcy porous cavity was investigated by (*Nguyen, et al.*, 2017 [19]) using the incompressible smoothed particle hydrodynamics (ISPH) method with the improved scheme for the wall boundary condition. The results showed that the higher amplitude and undulation number of the sinusoidal interface lead to a decrease in the average Nusselt number. (*Al-Zamily*, 2017 [20]) conducted a numerical study to analyze the natural convection inside a square enclosure with internal heat generation. The enclosure is divided into three layers, two sides layers occupied (TiO_2-Water) nanofluid while the third center layer is a porous medium occupied with the same nanofluid.

A vertically partially layered and differentially heated porous cavity filled with nanofluid has been considered by (*Chamkha* and *Ismael*, 2014 [21]), numerically. They considered double–domain formulation for their modeling, while the left and right walls were isothermally heated and cooled, respectively. The upper and lower walls were considered to be adiabatic. The Darcy–Brinkman model is used for the porous layer which is saturated with the same nanofluid. The governing equations are solved numerically. Five parameters are used to study; nanoparticle volume fraction (0–0.1), different porous layer thickness (0–0.9), Darcy number (10^{-7}–1), aspect ratio (1, 2, 4), and Rayleigh number Ra (10^3–10^6). The nanofluid (Cu-water). The results have shown that the convection heat transfer enhanced with the aid of nanofluid even at a low permeable porous medium. Also at Ra=10^5, there is a critical thickness of the porous layer at which the Nusselt number is maximum. Otherwise, the Nusselt number decreases rapidly with porous layer thickness. While, (*Madera, et al.*, 2011 [22]) have studied heat transfer in a parallel-plate channel partially filled with a porous. The heat transfer and momentum for the domain

problem were solved numerically by using the Finite Element Method (FEM). The simulations have been done in terms of different parameters: the porosity, the size of the porous insert, the Péclet number, and the thermal conductivity ratio. The results have revealed that increasing the size of the porous insert as well as favoring mixing inside the channel will improve the thermal performance. Another work by (*Chamkha* and *Aly*, 2010 [23]) focused on the boundary-layer flow analysis for a base pure fluid with nanoparticle additives along a porous vertical in the presence of the magnetic field. They also considered the heat generation or absorption as well as the suction or injection effects on their modeling. The model was solved by using the implicit finite-difference method. The results have shown that the existence of nanoparticles in the pure fluid had clear effects on both heat and mass transfer phenomena.

Enclosure partially filled with a vertical porous layer has been used (*Gobin, et al.*, 2005 [24]) to study the natural convection motivated by thermal and solutal buoyancy forces. The results showed the effect of the porous layer on both fluid structure and heat transfer in the cavity and both the flow penetration in the porous layer and the combined buoyancy forces achieved a specific treatment of the flow configuration and average heat transfer in the cavity.

Experimental and analytical natural convection heat transfer has been conducted (*Tatsuo et al.*, 1986 [25]) in a rectangular enclosure divided horizontally into porous (glass beads) and fluid regions (silicone oil), finite element method has been used to solve the Navier-stokes equation for range $10^3 \leq Ra \leq 10^5, 10^{-3} \leq Da \leq 10^{-5}$ with Brinkman's extension used for Darcy law. While, the effect of the fluid layer on Nusselt number in a vertical rectangular cavity has been analyzed experimentally and numerically by (*Beckermann et al.*, 1987 [26]). The porous layer (spherical glass beads) is modeled by Brinkman-Forchheimer-extended Darcy equations. The results have shown that the fluid penetrating into the porous layer is strongly dependent on both Darcy and Rayleigh numbers.

(*Arezou Jafari et al*., 2015(29)) conducted a numerical study by using CFD techniques to study the influence of gravity force on sedimentation on the natural convection of Ferro nanofluid in a disc shape. Magnetic force was applied as an external force. The results show that gravity forces boost the phase separation, sedimentation of ferrofluid, and natural convection heat transfer. (*Mohebbi Komeil et al.*, 2015(30)) examined a numerical study of forced convection turbulent flow inside a pipe having different rib configurations such as rectangular, trapezoidal, and semicircular. Trapezoidal and semi-circular have the highest heat transfer process than a rectangular shape. (*Amir Kaimdoost Yasuri et al.*, 2019(31)) investigated numerical work about free convection inside the enclosure having a square shape with a longitudinal baffle attached to the left wall. The enclosure was filled with Al_2O_3 nanofluids and H_2O as base fluid with a horizontal magnitude force effect. The result proves that the heat transfer rate increases with increasing Rayleigh number and baffle length and decreases with the presence of the magnetic field.

The main objective of the present numerical study investigation of the steady state heatlines analysis on the natural convection for multilayers of the nanofluid and porous medium and also, study the effect of a sinusoidal layer of the porous medium with the presence of the magnetic field. According to the literature review mentioned above and the authors' experiences, the studies in this work: analysis of heatlines, fluid flow, and heat transfer are examined for the first time since only reference (*Nguyen et al.*, 2017 [19]) studied the effect of permeability interface between a porous medium and nanofluid on the natural convection in a horizontally partitioned cavity. In addition, there was no inclusive work taking the influence of multi-parameters such as a number of undulations, Rayleigh number, Darcy number, Hartmann number, and volume fraction.

THEORETICAL SECTION

Geometry description and the governing equation

The geometric description of the present work is described in Fig. 1. It consists of a two-dimensional square enclosure with dimensions (L*L). The left side wall is kept at a constant hot temperature and the right wall is kept at a constant cold temperature, while the top and bottom walls are adiabatic. The enclosure is divided by a sinusoidal wall of thickness (L_{pm}=0.2L) into three layers. The left and the right layers (first and third layers) are occupied with (Cu-Water) nanofluid, while the middle sinusoidal layer (second layer) is a porous nanofluid filled with Cu-nanofluid. Three different cases corresponding to the number of undulation (N=1, 2, and 3) was explained. The surfaces between the porous layer and nanofluid layers are assumed permeable, while the other surfaces

Table 1. Thermophysical properties of pure water (Cu) nanoparticles (Hamida and Charrada 2014).

Properties	C_p(J/kg k)	ρ (kg/m^3)	k (W/m.k)	β(1/k)	μ (kg/m.s)
Copper (Cu)	385	8933	401	1.67×10^{-5}	-
Pure water	4179	997.1	0.613	21×10^{-5}	0.000372

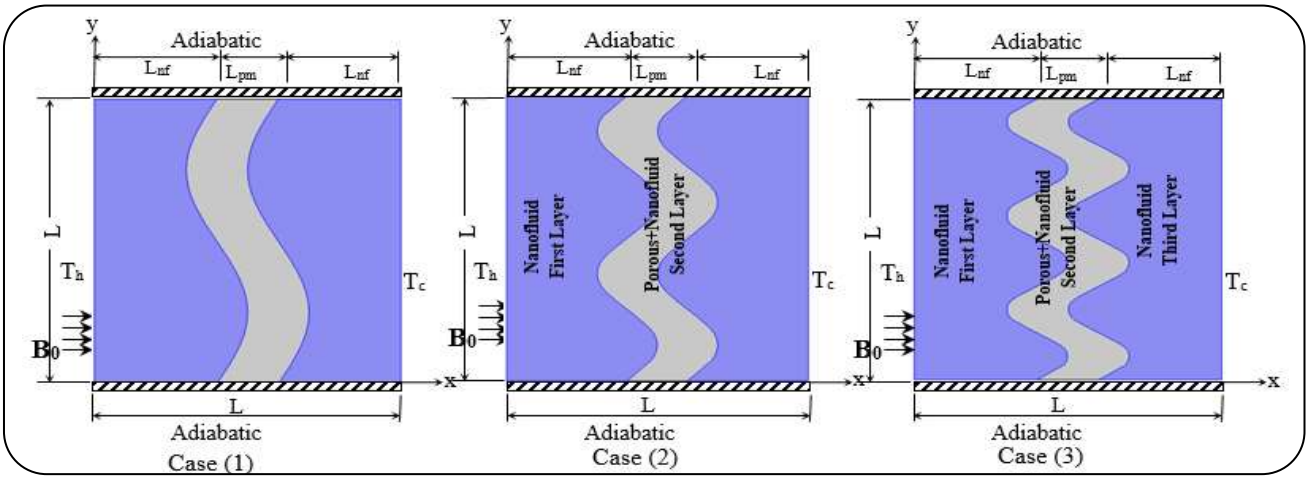

Fig. 1: Simplified diagram of the physical of the present study.

are assumed impervious. The spherical geometry has been assumed in terms of the shape and size of the nanoparticles, also, assumed the thermal balance between nanoparticles occupying the porous medium and solid substance.

The following assumptions are considered two-dimensional, steady state, laminar, Newtonian, with constant thermophysical properties except for the density which changes with temperature, allowing for Boussinesq approximation, no heat generation, and neglecting radiation. Moreover, the nanofluid consist of a base fluid (water) and solid particles (Cu). The thermophysical properties of Cu-Water nanofluid which are studied in the present study are specified in Table 1.

In the present study, the double domain method is used to find the mathematical model. The governing equations are extracted and presented for both domains. Both domains are connected with appropriate boundary conditions besides the permeable surfaces. In this study, Darcy-Brinkman model is considered to signify the convection inside the porous area. This model was summarized to simplify and couple the momentum equation between the nanofluid and porous domains. The governing equations for the nanofluid field (First & Third layers) in dimensional shape are *(Hussain and Rahomey*, 2018(18), *Al-Zamily*, 2017 [20]):

$$\text{Continuity} \quad \frac{\partial u_{na}}{\partial x} + \frac{\partial v_{na}}{\partial y} = 0 \tag{1}$$

$$\text{X-momentum} \quad \rho_{na}\left(u_{na}\frac{\partial u_{na}}{\partial x} + v_{na}\frac{\partial u_{na}}{\partial y}\right) = -\frac{\partial p}{\partial x} + \mu_{na}\left(\frac{\partial^2 u_{na}}{\partial x^2} + \frac{\partial^2 u_{na}}{\partial y^2}\right) \tag{2}$$

$$\text{Y-momentum} \quad \rho_{na}\left(u_{na}\frac{\partial v_{na}}{\partial x} + v_{na}\frac{\partial v_{na}}{\partial y}\right) = -\frac{\partial p}{\partial x} + \mu_{na}\left(\frac{\partial^2 u_{na}}{\partial x^2} + \frac{\partial^2 u_{na}}{\partial y^2}\right) + \beta_{na}\rho_{na}g\left(T_h - T_c\right) \tag{3}$$

$$\text{Energy} \quad u_{na}\frac{\partial T_{na}}{\partial x} + v_{na}\frac{\partial T_{na}}{\partial y} = \left(\frac{\partial^2 T_{na}}{\partial x^2} + \frac{\partial^2 T_{na}}{\partial y^2}\right) \tag{4}$$

The 2-D governing equations for the porous media area (Second layer) are:

$$\text{Continuity} \quad \frac{\partial u_{po}}{\partial x} + \frac{\partial v_{po}}{\partial y} = 0 \tag{5}$$

$$X-momentum \quad \rho_{na}\left(u_{po}\frac{\partial u_{po}}{\partial x}+v_{po}\frac{\partial u_{po}}{\partial y}\right)= \tag{6}$$

$$-\varepsilon^2\frac{\partial p}{\partial x}+\varepsilon\mu_{na}\left(\frac{\partial^2 u_{po}}{\partial x^2}+v_{po}\frac{\partial^2 u_{po}}{\partial y^2}\right)-\varepsilon^2\frac{\mu_{na}}{k}u_{po}$$

$$Y-momentum \quad \rho_{na}\left(u_{po}\frac{\partial v_{po}}{\partial x}+v_{po}\frac{\partial v_{po}}{\partial y}\right)= \tag{7}$$

$$-\varepsilon^2\frac{\partial p}{\partial y}+\varepsilon\mu_{na}\left(\frac{\partial^2 v_{po}}{\partial x^2}+\frac{\partial^2 v_{po}}{\partial y^2}\right)-\varepsilon^2\frac{\mu_{na}}{k}u_{po}+$$

$$\beta_{na}\rho_{na}g\left(T-T_c\right)-\sigma_{fl}B_o^2 v_{po}$$

$$Energy \quad u_{po}\frac{\partial T_{po}}{\partial x}+v_{po}\frac{\partial T_{po}}{\partial y}= \tag{8}$$

$$\alpha_{eff}\left(\frac{\partial^2 T_{po}}{\partial x^2}+\frac{\partial^2 T_{po}}{\partial y^2}\right)$$

Where ρ is density, α refers to thermal diffusivity, μ shows the dynamic viscosity, ε is porosity, K denotes permeability and β represents the thermal expansion coefficient. *na*, *po*, *fl* are the subscripts that indicate the nanofluid, porous medium, and pure fluid, respectively. Suppose the stream function is ($u=\frac{\partial\psi}{\partial y}$), ($v=-\frac{\partial\psi}{\partial x}$) and vorticity ($\omega=\frac{\partial v}{\partial x}-\frac{\partial u}{\partial y}$) and defining the dimensionless parameters as follows:

$$X=\frac{x}{L};\quad Y=\frac{y}{L};\quad U=\frac{uL}{\alpha_{fl}};\quad V=\frac{vL}{\alpha_{fl}};\quad P=\frac{pL^2}{\rho_{na}\alpha_{fl}^2};$$

$$Da=\frac{k_{fl}}{L^2};\ \theta=\frac{T-T_c}{T_h-T_c}$$

$$Ra=\frac{g\beta_{fl}\left(T_h-T_c\right)L^3}{\nu_{fl}\alpha_{fl}},\ Pr=\frac{\nu_{fl}}{\alpha_{fl}},\ \Psi=\frac{\psi}{\alpha_{fl}},\ \Omega=\frac{\omega L^2}{\alpha_{fl}},$$

$$Ha=B_o L\sqrt{\frac{\sigma_{fl}}{\mu_{fl}}}$$

The physical properties of the nanofluid can be considered by the following equations [3]:

$$\rho_{na}=(1-\varphi)\rho_{fl}+\varphi\rho_{po} \tag{9}$$

$$(\rho\beta)_{na}=(1-\varphi)(\rho\beta)_{fl}+\varphi(\rho\beta)_{po} \tag{10}$$

$$\alpha_{na}=\frac{K_{na}}{\left(\rho c_p\right)_{na}} \tag{11}$$

$$\alpha_{eff}=\frac{K_{eff}}{\left(\rho c_p\right)_{na}} \tag{12}$$

$$K_{eff}=(1-\varepsilon)K_s+\varepsilon K_{na} \tag{13}$$

$$\left(\rho c_p\right)_{na}=(1-\varphi)\left(\rho c_p\right)_{fl}+\varphi\left(\rho c_p\right)_{po} \tag{14}$$

$$K_{na}=K_{fl}\frac{\left(K_{po}+2K_{fl}\right)-2\varphi\left(K_{fl}-K_{po}\right)}{\left(K_{po}+2K_{fl}\right)+2\varphi\left(K_{fl}-K_{po}\right)} \tag{15}$$

$$\mu_{na}=\frac{\mu_{fl}}{(1-\varphi)^{2.5}} \tag{16}$$

The dimensionless governing equations for the nanofluid domain (First & Third layers) take the form as follows:

$$Continuity \quad \frac{\partial U_{na}}{\partial X}+\frac{\partial V_{na}}{\partial Y}=0 \tag{17}$$

$$X-momentum \quad U_{na}\frac{\partial U_{na}}{\partial X}+V_{na}\frac{\partial U_{na}}{\partial Y}= \tag{18}$$

$$-\frac{\partial P}{\partial X}+\frac{Pr}{(1-\varphi)^{2.5}}\frac{\rho_{fl}}{\rho_{na}}\left(\frac{\partial^2 U_{na}}{\partial X^2}+\frac{\partial^2 U_{na}}{\partial Y^2}\right)$$

$$Y-momentum \quad U_{na}\frac{\partial V_{na}}{\partial X}+V_{na}\frac{\partial V_{na}}{\partial Y}= \tag{19}$$

$$-\frac{\partial P}{\partial X}+\frac{Pr}{(1-\varphi)^{2.5}}\frac{\rho_{fl}}{\rho_{na}}\left(\frac{\partial^2 V_{na}}{\partial X^2}+\frac{\partial^2 V_{na}}{\partial Y^2}\right)+$$

$$\frac{(\rho\beta)_{na}}{\rho_{na}\beta_{fl}}Ra\,Pr\,\theta-\frac{\rho_{fl}}{\rho_{na}}\frac{\sigma_{na}}{\sigma_{fl}}Ha^2\,Pr\,\nu_{na}$$

$$Energy \quad U_{na}\frac{\partial\theta_{na}}{\partial X}+V_{na}\frac{\partial\theta_{na}}{\partial Y}= \tag{20}$$

$$\frac{\alpha_{na}}{\alpha_{fl}}+\left(\frac{\partial^2\theta_n}{\partial X^2}+\frac{\partial^2\theta_n}{\partial Y^2}\right)$$

The dimensionless form of the governing equations for the porous media area (Second layer) is:

$$Continuity \quad \frac{\partial U_{po}}{\partial X}+\frac{\partial V_{po}}{\partial Y}=0 \tag{21}$$

$$X-momentum \quad U_{po}\frac{\partial U_{po}}{\partial X}+V_{po}\frac{\partial U_{po}}{\partial Y}= \tag{22}$$

$$-\frac{\partial P}{\partial X}+\frac{Pr}{(1-\varphi)^{2.5}}\frac{\rho_{fl}}{\rho_{na}}\left(\frac{\partial^2 U_{po}}{\partial X^2}+\frac{\partial^2 U_{po}}{\partial Y^2}\right)-$$

$$\frac{Pr}{(1-\varphi)^{2.5}}\frac{\rho_{fl}}{\rho_{na}}\frac{U_{po}}{Da}$$

$$X-momentum \quad U_{po}\frac{\partial V_{po}}{\partial X}+V_{po}\frac{\partial V_{po}}{\partial Y}= \tag{23}$$

$$-\frac{\partial P}{\partial X}+\frac{Pr}{(1-\varphi)^{2.5}}\frac{\rho_{fl}}{\rho_{na}}\left(\frac{\partial^2 V_{po}}{\partial X^2}+\frac{\partial^2 V_{po}}{\partial Y^2}\right)-$$

$$\frac{Pr}{(1-\varphi)^{2.5}}\frac{\rho_{fl}}{\rho_{na}}\frac{V_{po}}{Da}+\frac{(\rho\beta)_{na}}{\rho_{na}\beta_{fl}}Ra\,Pr\,\theta-\frac{\rho_{fl}}{\rho_{na}}\frac{\sigma_{po}}{\sigma_{fl}}Ha^2\,Pr\,v_{po}$$

$$Energy \quad U_{po}\frac{\partial \theta_{po}}{\partial X}+V_{po}\frac{\partial \theta_{po}}{\partial Y}= \tag{24}$$

$$\frac{\alpha_{na}}{\alpha_{fl}}\left(\frac{\partial^2 \theta_{po}}{\partial X^2}+\frac{\partial^2 \theta_{po}}{\partial Y^2}\right)$$

The boundary conditions on the outside walls of the enclosure are:

At X=0 U=V=Ψ=0, θ=1 (left side wall)

At X=1 U=V=Ψ=0, θ=0 (right side wall)

At Y=0 U=V=Ψ=0, $\frac{\partial\theta}{\partial X}=0$ (adiabatic bottom wall)

At Y=1 U=V=Ψ=0, $\frac{\partial\theta}{\partial x}=0$ (adiabatic top all)

The conditions were considered for the permeable sinusoidal surfaces between the porous domain and nanofluid as follows:

$$\theta_{po}=\theta_{na}\ ,\ \frac{\partial\theta_{na}}{\partial n}=\frac{K_{eff}}{K_{na}}\frac{\partial\theta_{po}}{\partial n}\ , \tag{25}$$

$$\Psi_{po}=\Psi_{na}\ ,\ \frac{\partial\Psi_{na}}{\partial n}=\frac{\partial\Psi_{po}}{\partial n}\ ,$$

$$\Omega_{po}=\Omega_{na}\ ,\ \frac{\partial\Omega_{na}}{\partial n}=\frac{\partial\Omega_{po}}{\partial n}\ ,$$

$$\mu_{po}\left(\frac{\partial U_{po}}{\partial Y}+\frac{\partial V_{po}}{\partial X}\right)=\mu_{na}\left(\frac{\partial U_{na}}{\partial Y}+\frac{\partial V_{na}}{\partial X}\right),$$

$$P_{po}=P_{na}\ ,\ \frac{\partial P_{po}}{\partial n}+\frac{\partial P_{na}}{\partial n}$$

The local and average Nusselt number for the hot wall can be written in the shape of

$$Nu_{local}=\frac{K_{na}}{K_{fl}}\frac{\partial\theta}{\partial n}\quad,\quad Nu_{ave}=\frac{K_{na}}{K_{fl}}\int_0^1\frac{\partial\theta}{\partial n}dy \tag{26}$$

The stream function was obtained from velocity segments U and V to describe the fluid motion inside the enclosure. The relation between velocity segments and stream function are:

$$U=\frac{\partial\Psi}{\partial Y}\quad,\quad V=\frac{\partial\Psi}{\partial X} \tag{27}$$

$$\frac{\partial^2\Psi}{\partial X^2}+\frac{\partial^2\Psi}{\partial Y^2}=\frac{\partial U}{\partial Y}-\frac{\partial V}{\partial X} \tag{28}$$

On the other side; the heatlines visualization is expressed by the following mathematical relation. The heat function is composed of heat conduction $(-\frac{\partial\theta}{\partial X},-\frac{\partial\theta}{\partial Y})$ and heat convection (Uθ, Vθ) (Al-Zamily, 2017 [20])

$$\frac{\partial\Pi}{\partial Y}=U\theta\frac{\alpha_{na}}{\alpha_{fl}}\frac{\partial\theta}{\partial X}\quad,\quad-\frac{\partial\Pi}{\partial X}=V\theta-\frac{\alpha_{na}}{\alpha_{fl}}\frac{\partial\theta}{\partial Y} \tag{29}$$

The heat function relation was obtained from the energy balance equation, as follows:

$$\frac{\partial^2\Pi}{\partial X^2}+\frac{\partial^2\Pi}{\partial Y^2}=\frac{\partial}{\partial Y}(U\theta)-\frac{\partial}{\partial X}(V\theta) \tag{30}$$

Numerica; procedure, grid independence, and code validation

The dimensionless governing equations are solved using the Galerkin Finite Element method to obtain the temperature and stream function contours, based on the weak formulation. The mesh used in the present study for two dimensional is triangular elements with a non-uniform distribution. The mesh distribution can be noticed in Fig. 2, and graduate for computational fluid dynamics. Many grid sensibility checks were carried out to find the mesh stability and to guarantee that the solution is grid independency listed in Table 2. The table includes the mesh size, mesh elements, boundary elements, average Nusselt number, and the time elapsed for each mesh size. The extreme fine mesh is chosen which gives accurate results. To confirm the code calculations, the comparison with an antecedently published article on natural convection in a square enclosure filled with ethylene Glycol-coppe nanofluid under a magnetic field (*Hamida* and *Charrada*, 2014 [27]).

Table 2: Grid sensitivity check for the case $Ra=10^5$, $Da=0.001$ and $Ha=20$, $\varphi=0.05$.

Mesh size	Mesh elements	Boundary elements	$\overline{Nu}$	CPU time sec
Fine	2418	208	3.4561	5
Finer	6268	400	3.4370	9
Extra fine	16646	744	3.4159	18
Extremely fine	25678	792	3.4111	25

Table 3: Comparison of the average Nusselt number between the present and Hamida and Charrada, 2014 [27], the result for a different for different Hartmann numbers at solid volume fraction $\varphi= 0.05$, $Ra=10^5$, (ethylene glycol–Cu nanofluid).

	Mean Nusselt number at the hot wall		Error(%)
Ha	Present study	Hamida and Charrada,2014 [27],	
0	5.1031	5.0	-2.062
20	3.8135	3.8	-0.355
40	2.4274	2.4	-1.141
60	1.7262	1.7	-1.541
80	1.4185	1.4	-1.321
100	1.2859	1.3	1.084

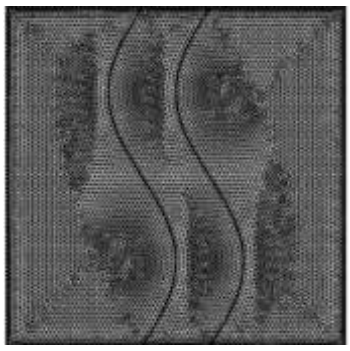

Fig. 2: Mesh Distribution of the Model.

The comparison was made in heat transfer by average Nusselt number as in Table 3 and fluid flow with temperature distribution as in Fig. 3. The comparison showed the sure result to calculate the exactness of the present numerical study.

RESULTS AND DISCUSSION

The outcomes of the present research are depicted and discussed for different Rayleigh numbers **(10^3-10^6),** Darcy number range **(10^{-1}-10^{-5}),** nanoparticles volume fraction range **(0-0.06),** and Hartmann Number Range **(0-100).** The porous layer has a wavy shape with a different amplitude (single, two, and three), while the porosity is fixed at **ε=0.398** corresponds to a glass bed of thermal conductivity =**0.845** W/m.K

In this section, the database results are shown in terms of Headlines, Isothermal lines, Streamfunction, and local and average Nusselt numbers for three cases depending on the number of wavy porous layers.

Heatlines and isothermal lines

In two-dimensional convective transport systems, the heatline is the best technique to illustrate heat transmission. The best tools for visualizing fluid dynamics in two-dimensional incompressible flow are streamlines. Heatlines, which also heat flux lines, show the course of heat energy in a similar way. In general, the heat flux lines for heat transfer owing to pure conduction through the isotropic medium are normal to the isotherms. Heatlines can best illustrate energy flow within multiple regimes, notably for convective heat transport processes, but isotherms are unable to provide guidance for energy fluxes. The heatlines are mathematically represented by heat functions and the proper dimensionless forms of heat functions are closely related to overall Nusselt numbers.

The heatlines and isotherms for three cases of the wavy porous medium at the Hartmann number range **(0-100),** constant Rayleigh number **=10^5**, nanoparticles volume

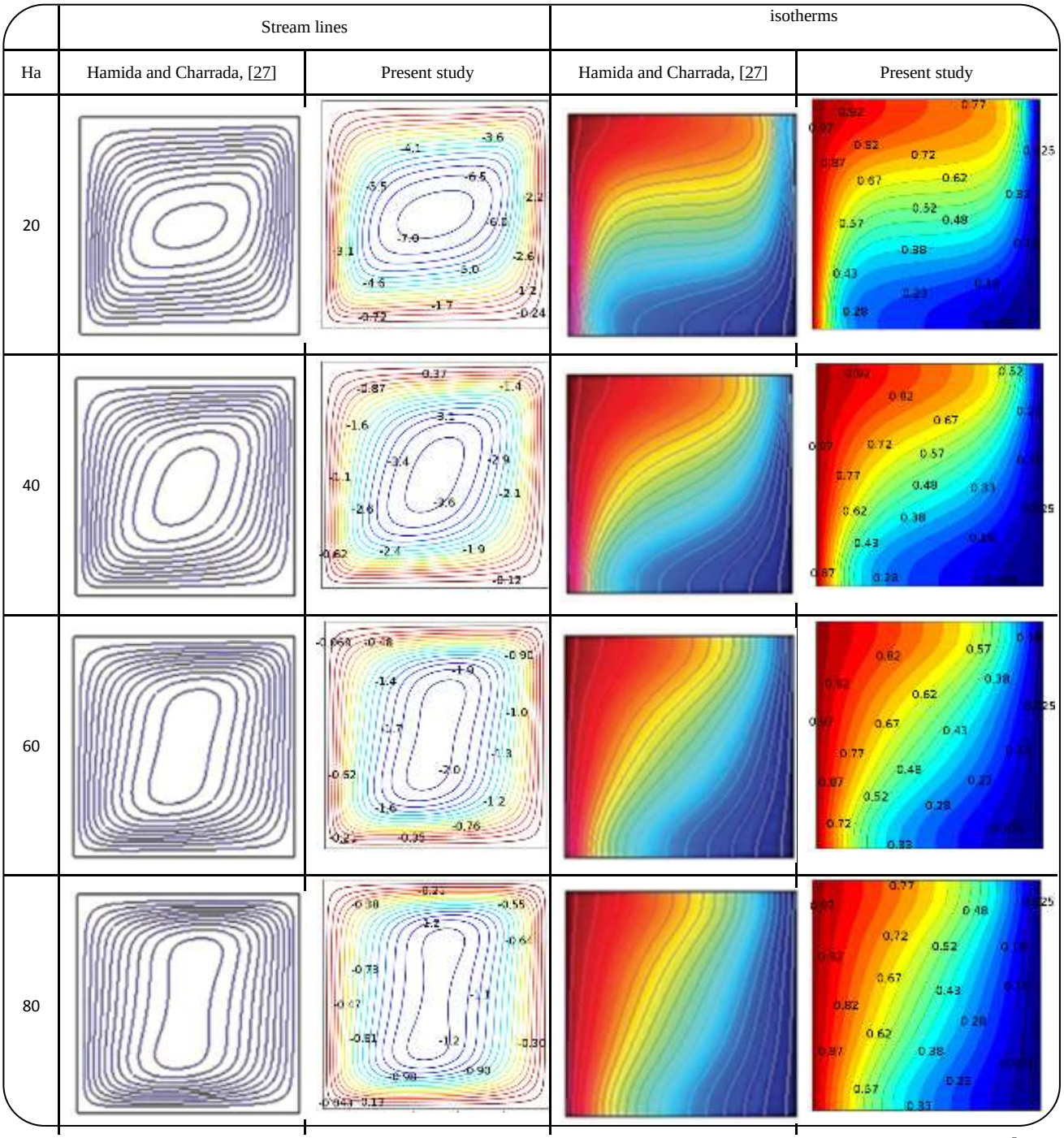

Fig. 3: Streamlines(left), and Isotherms (right) for different Hartmann numbers at solid volume fraction φ= 0.05, Ra=10^5, (ethylene glycol–Cu nanofluid). For Hamida and Charrada,2014 [27], and the present study.

fraction =**0.05,** and Darcy number=**0.1** plot in **Fig. 4.** In this figure, it can be shown for the three cases, heatlines are started from the hot surfaces with the direction of the magnetic field and ended with the cold one. A circular heatlines will be observed ***(i.e. the convection effect is great).*** The circular heatlines reduces as the Hartmann number increase. The core center of the circular heatlines moves toward the wavy porous partition and increases as the amplitude increase. Furthermore, the central shape varies from an elliptical shape to the circular one as the Hartmann number increases. The circular heatlines are located centrally at **Ha=0** and move toward the lower left corner as the Hartmann number increase. As the Darcy number

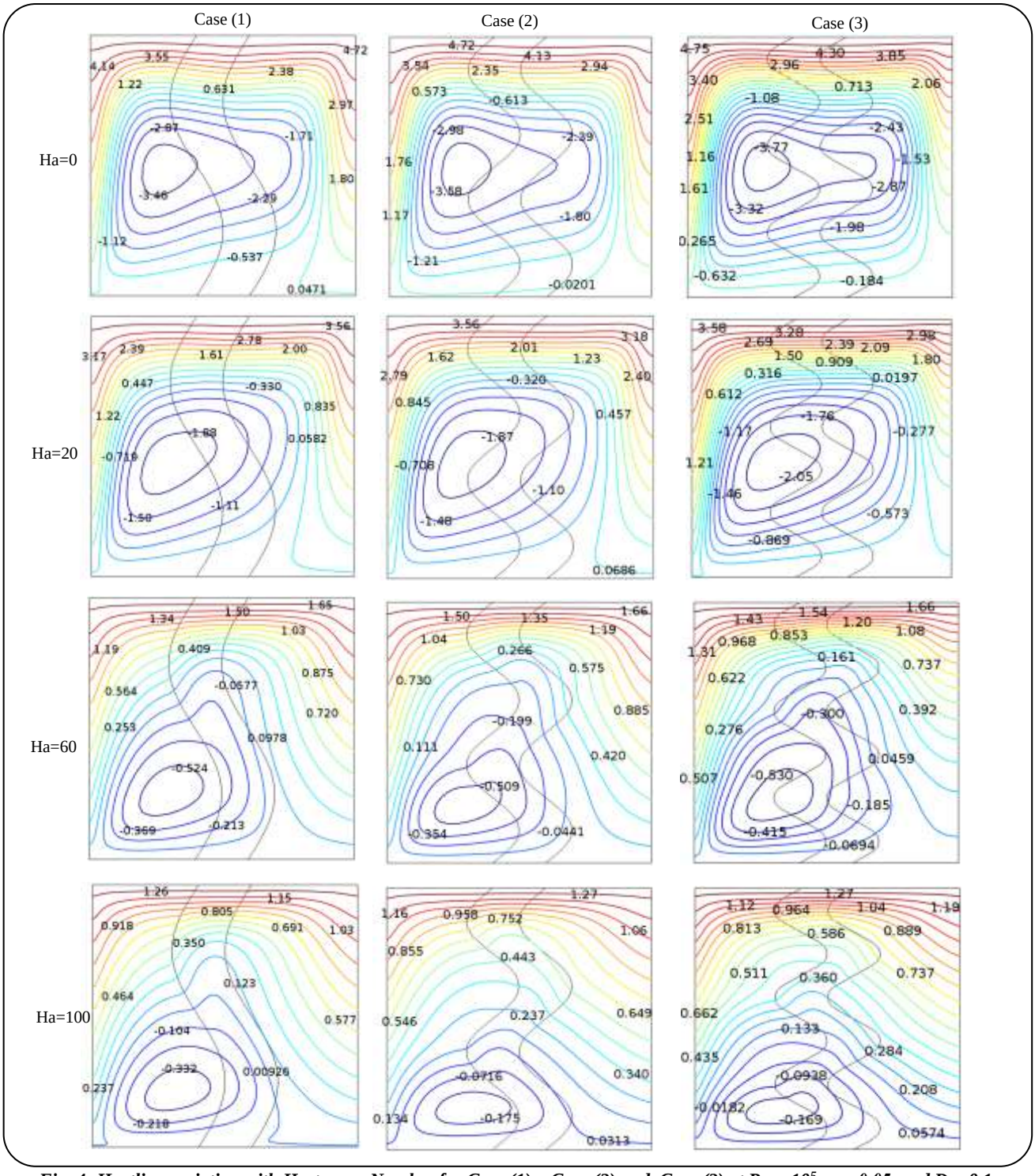

Fig. 4: Heatline variation with Hartmann Number for Case (1). , Case (2) and Case (3) at Ra = 10^5, φ = 0.05, and Da=0.1.

in the wavy porous domain layer is reduced, the circular heatlines vanish due to the increase in the conduction effect ***(i.e. the heatlines became perpendicular to the isothermal lines)*** which is shown in **Fig. 5.** The Darcy number effect on the heatlines is very obvious in **Fig. 6** at **Ha=0** produced two circular heatlines as the amplitude of the wavy porous media increase due to an increase in conduction heat transfer than convection since the porous layer work as restricted

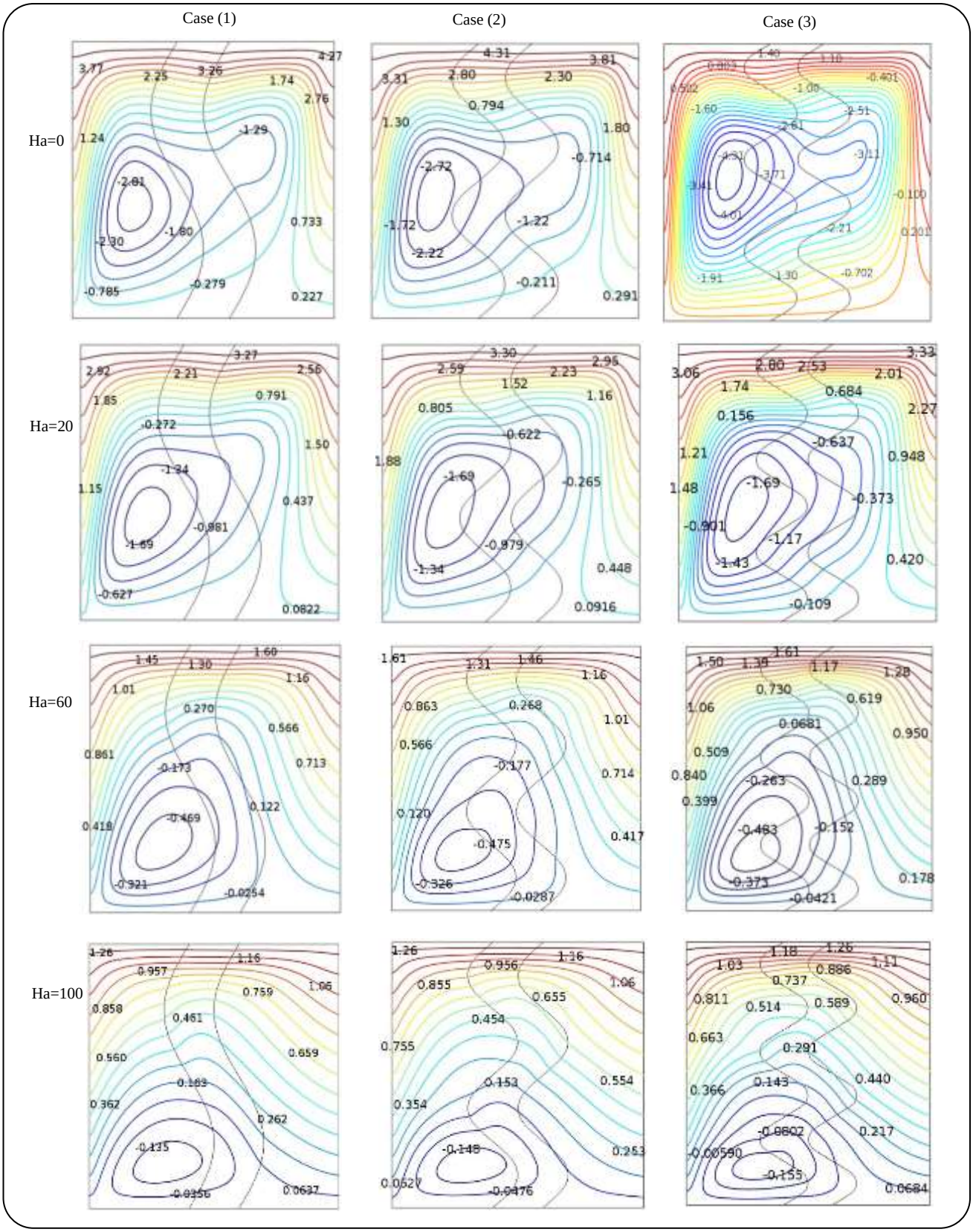

Fig. 5: Heatline variation with Hartmann Number for Case (1). ,Case (2) and Case (3) at Ra = 10^5, φ = 0.05 and Da=0.001.

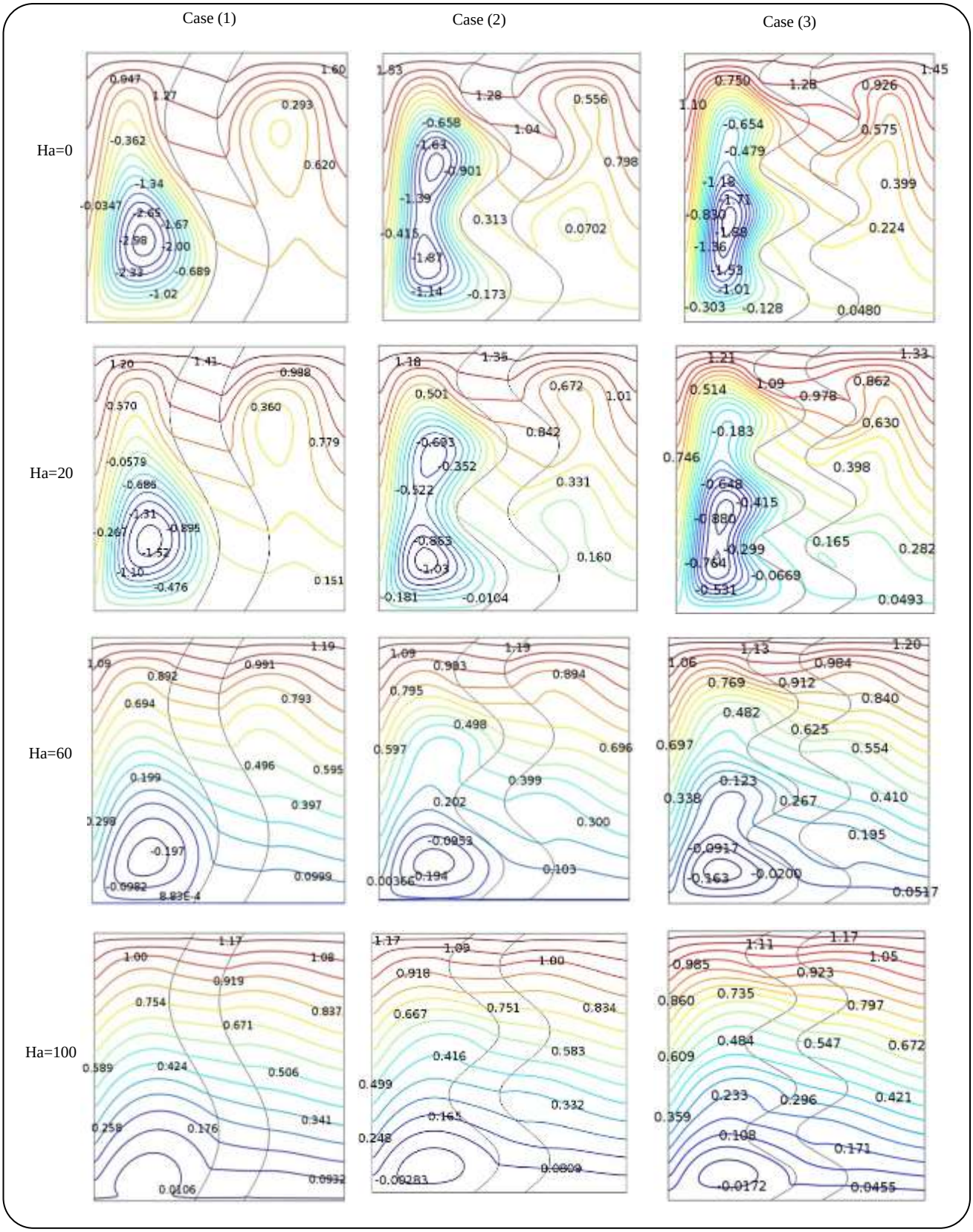

Fig. 6: Heatline variation with Hartmann Number for Case (1). ,Case (2) and Case (3) at Ra = 10^5, φ = 0.05 and Da=0.00001.

wall ***(solid wall).*** The Hartmann number effect on the heatlines value depends on the Darcy number at a high Rayleigh number such as at **$Ra=10^5$, $\phi=0.05$** the decreases in the peak values of heart function due to the magnetic field **(Ha=100)** as follows

*-for single wavy porous media: (1.316) at Da=0.1, (1.3047) at Da=0.001, (1.2085) at Da=0.00001

*-for two wavy porous media: (1.7366) at Da=0.1, (1.3047) at Da=0.001, (1.2085) at Da=0.00001

*-for three wavy porous media: (1.3042) at Da=0.1, (1.2945) at Da=0.001, (1.2046) at Da=0.00001

The Darcy number also affects the isothermal lines as appears very clear in **Figs. 7-9.** The convection heat transfer effect is reduced as the Darcy number reduced and the heat transfer inside the wavy porous media layer occurs by conduction so, the slope of the isothermal lines decreases and became perpendicular to the heatlines as the Darcy number decreases and Hartmann increases for all three cases. At $Da=10^{-1}$, there was no noticeable effect of the wavy porous medium resistance, and the convective heat transfer dominated both nanofluid and wavy porous layers and the nanoparticles become to affect the streamlines, particularly in the porous layer at $Da=10^{-1}$ as shown in Fig. 7 and Fig. 8. While, in Fig. 9 the $Da=10^{-5}$ so the wavy porous medium layers act like a rigid wall that prevents the nano-fluid from penetrating it, and the convective heat transfer is restricted in only the nano-fluid layer bounded by the wavy nano-fluid/porous wavy medium interface, whereas the convective heat transfer dominates the wavy porous layer. The slope of the isotherms decrease as the Hartmann number increased and became perpendicular on heatlines as shown in all Figures above.

Stream function

Since the fluid near the hot surfaces is hotter than the other fluid so, the density is reduced and driven upward, then moved toward the cold surfaces. ***(i.e. this process creates clockwise circular streamlines that control the flow inside the enclosure)*** as shown in **Figs. 10-12.** At **Da=0.1** and **Ha=0**, the core contour of the streamlines became uniform and located near the center of gravity, but as the number of wavy porous media layers increased, the circular stream function moves toward the cold surfaces. As the Hartmann number increased the circular core of the stream function became longitudinally at the wavy porous layer due to the increases in the penetration of fluid through the wavy porous layer as shown in **Figs. (10, 11).**

In **Fig. 12,** it can be shown at a low Darcy number**=0.00001** and for single wavy porous at all numbers of Hartmann, two stream functions produced in the first and third nanofluid layers due to a low fluid penetration by the single wavy porous sheet and a high hydrodynamics resistance by the porous medium.

While, as the wavy porous layer increased from single to second and third amplitude producing two stream functions in the first and third nanofluid layers, each one with two cores due to the reduced penetration of fluid through the second porous sheet as compared with the fluid flow in the first and third nanofluid layers. Also, the Darcy and Hartmann numbers affect the absolute value of the stream function as shown in **Fig. 10-12** as the Darcy number increases the absolute value of the maximum stream function growth due to the increase in fluid movement and high penetration of nanofluid through the wavy porous layer. While, as the Hartmann number rises the value of the absolute maximum stream function decreased due to the increase in the hydrodynamic resistance which reduced the fluid movement.

Nusselt number

Since the average Nusselt number can be considered as one of the main factors that give the indicator of the heat transfer so, the local Nusselt number along the hot wall plot in **Fig. 13** for two cases **(Da=0.001 and Da=0.00001)** and a different Hartmann number. It can be presented that the local Nusselt number reduces along the hot wall as the Hartmann number increased at a high Darcy number due to the increased penetration of nanofluid through a wavy porous layer to the cold surface. Also, the effect of the Rayleigh number on the local Nusselt number it can be shown in **Fig. 14** for three cases of the wavy porous layer and two values of Darcy number with a constant Hartmann number**=20**. It can be shown that the local Nusselt number increases as the Rayleigh number increase even though the Darcy number is high due to the increase in fluid movement in the nanofluid layer which increases consequently the convection heat transfer, but conduction heat transfer still happens in the wavy porous domain due to a relatively high hydrodynamic resistance at **Da=0.00001**.

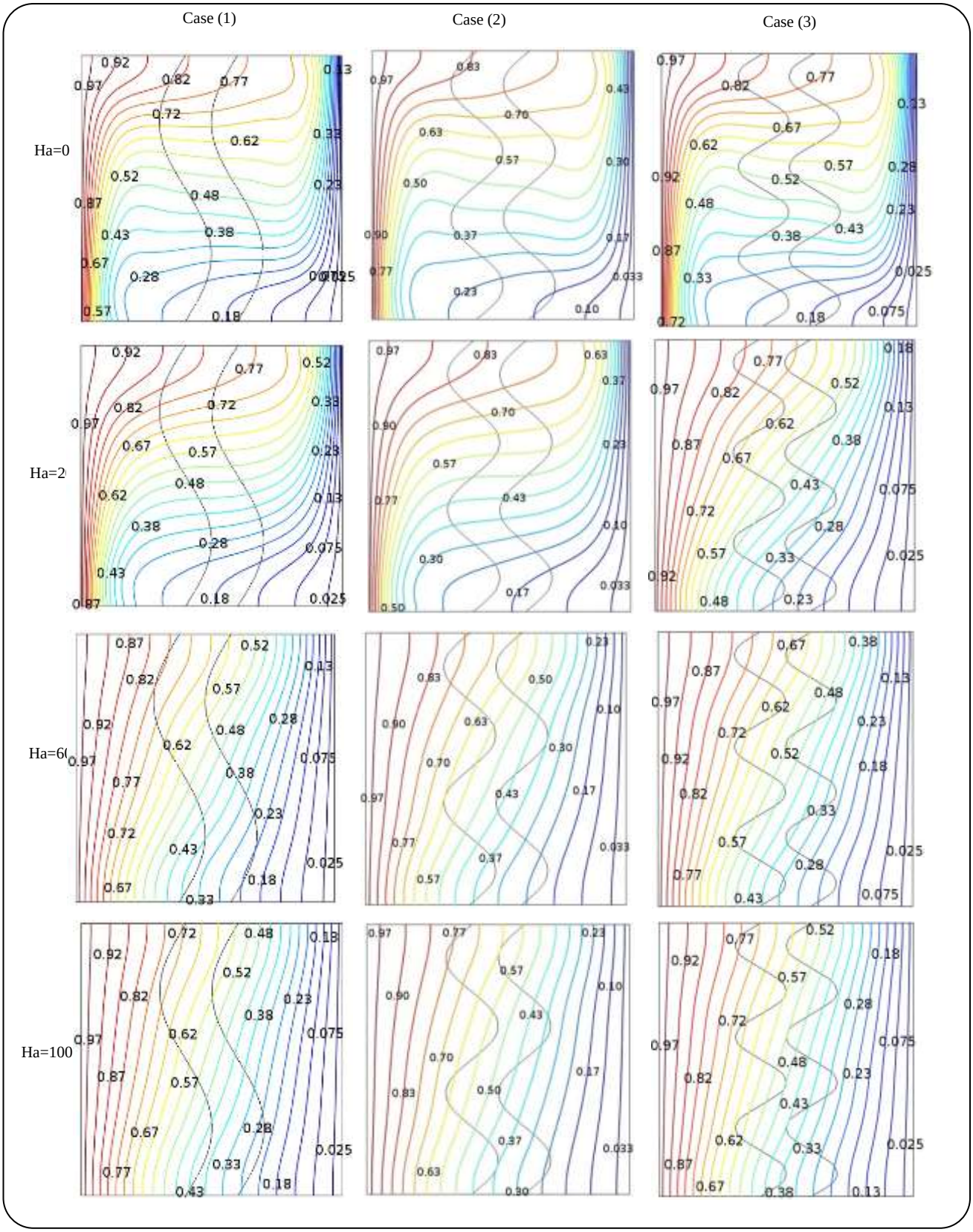

Fig. 7: Isotherms variation with Hartmann Number for Case (1). , Case (2) and Case (3) at Ra = 10^5, φ = 0.05, and Da=0.1.

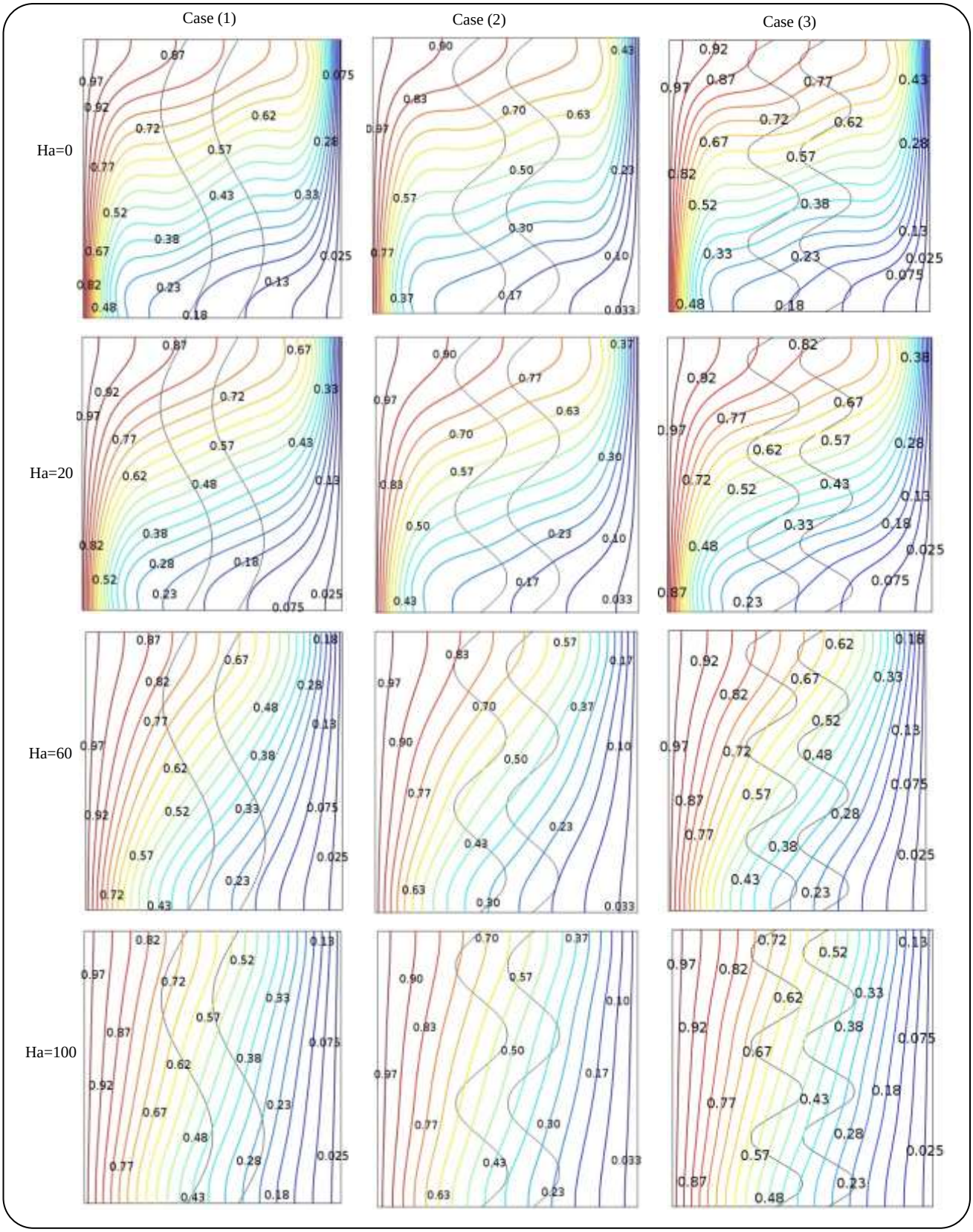

Fig. 8: Isotherms variation with Hartmann Number for Case (1). , Case (2) and Case (3) at Ra = 10^5, φ = 0.05, and Da=0.001.

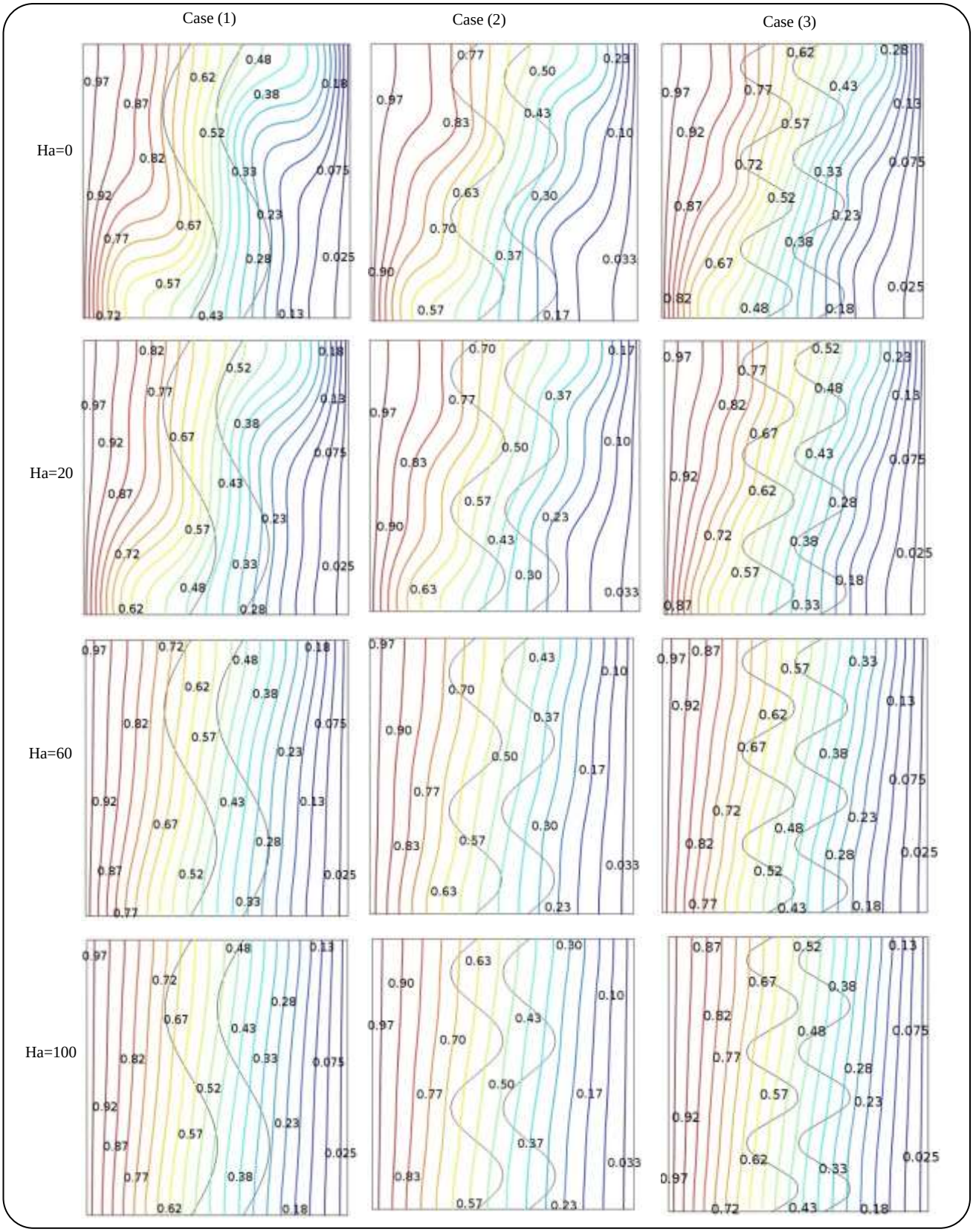

Fig. 9: Isotherms variation with Hartmann Number for Case (1). , Case (2) and Case (3) at Ra = 10^5, φ = 0.05, and Da=0.00001.

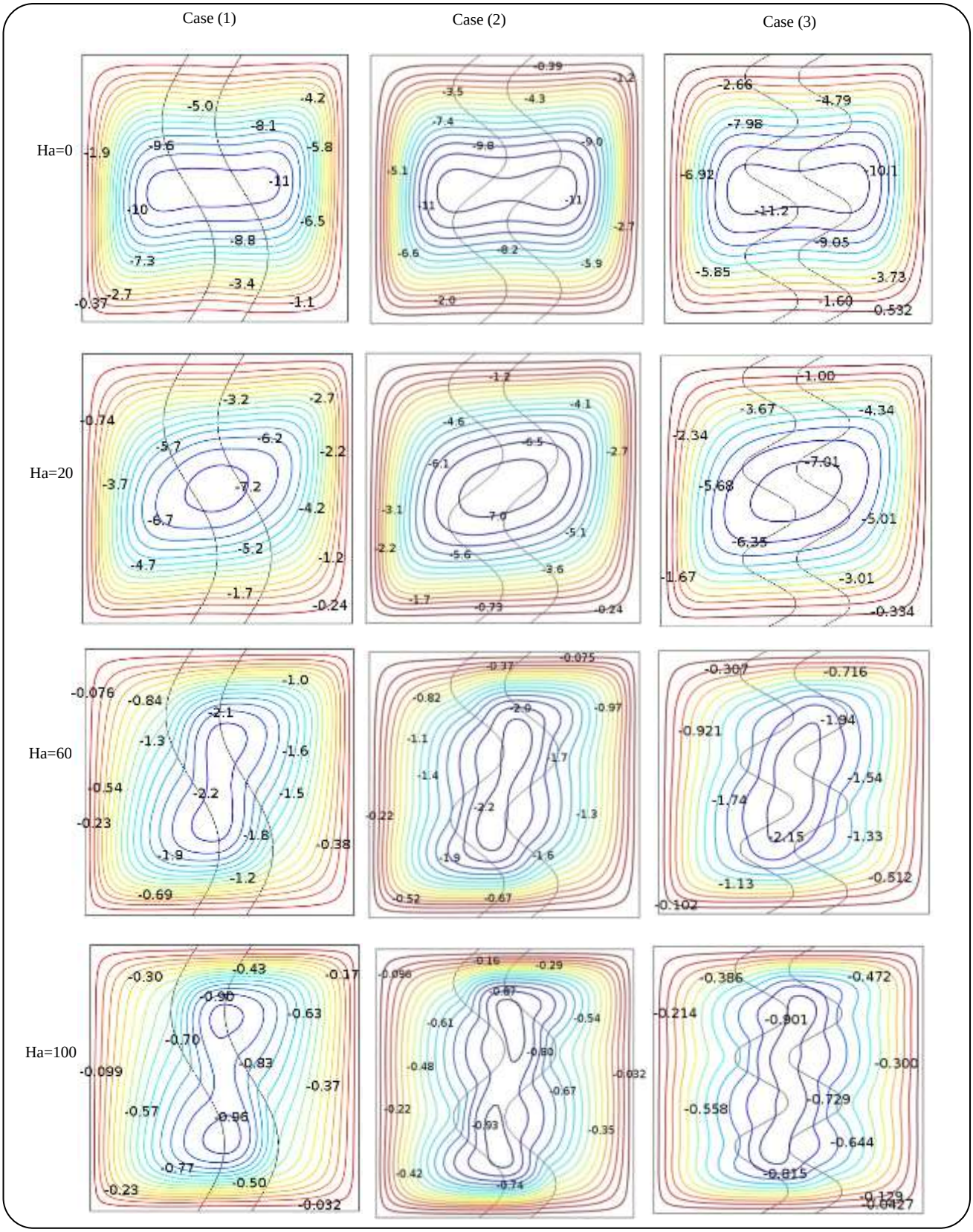

Fig. 10: Streamlines variation with Hartmann Number for Case (1). , Case (2) and Case (3) at Ra = 10^5, φ = 0.05, and Da=0.1.

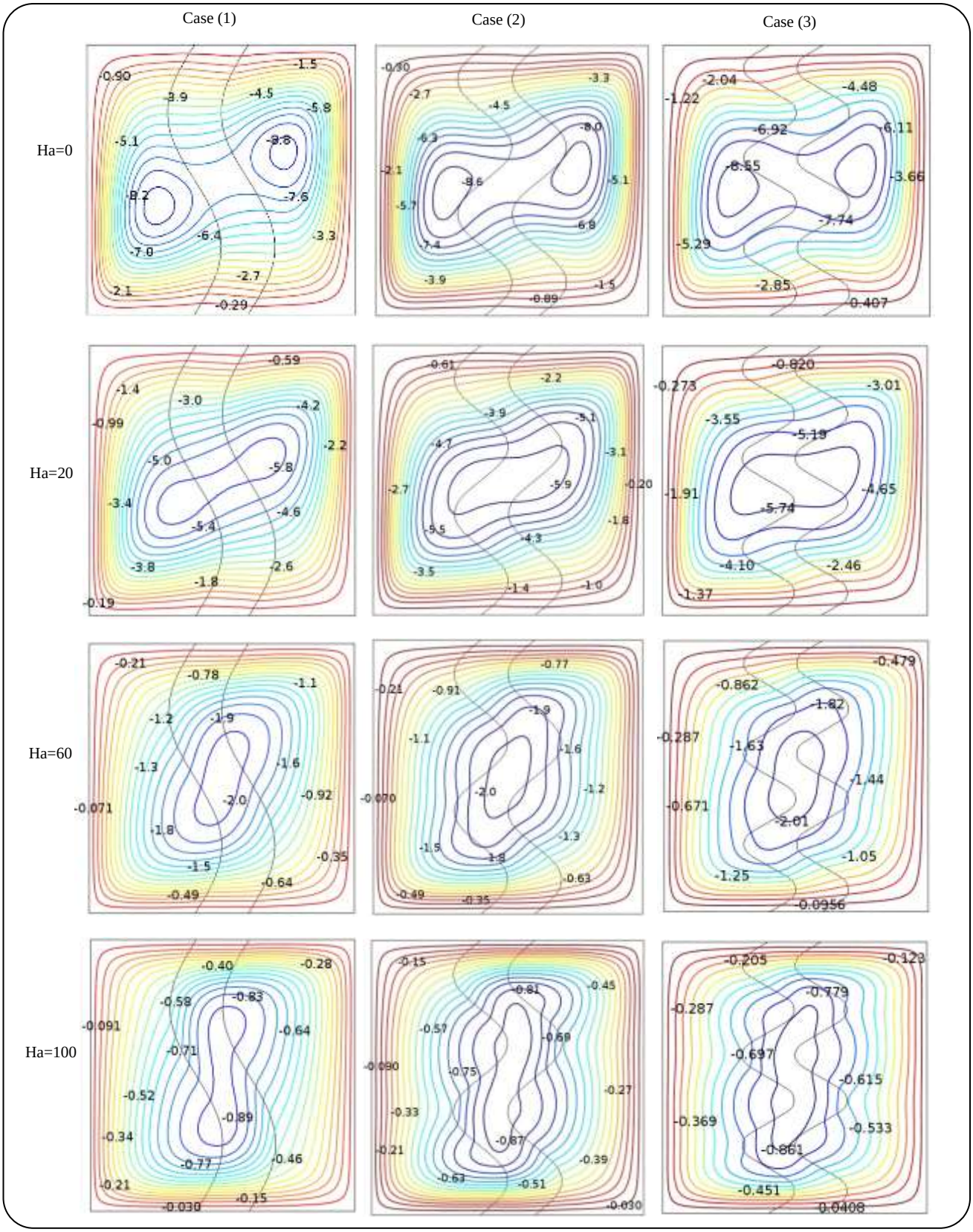

Fig. 11: Streamlines variation with Hartmann Number for Case (1). , Case (2) and Case (3) at Ra = 10^5, φ = 0.05, and Da=0.001.

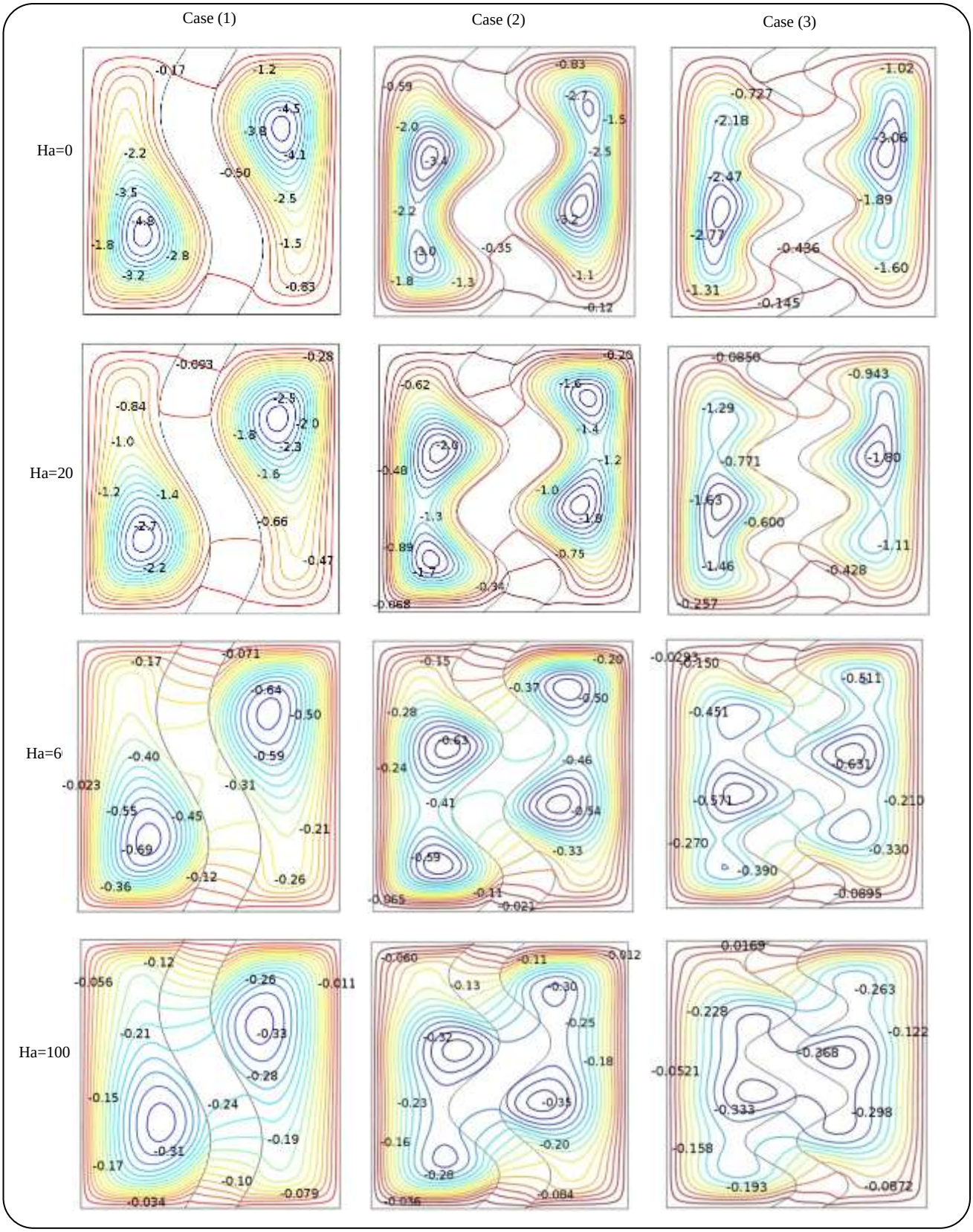

Fig. 12: Streamlines variation with Hartmann Number for Case (1). , Case (2) and Case (3) at Ra = 10^5, φ = 0.05, and Da=0.00001.

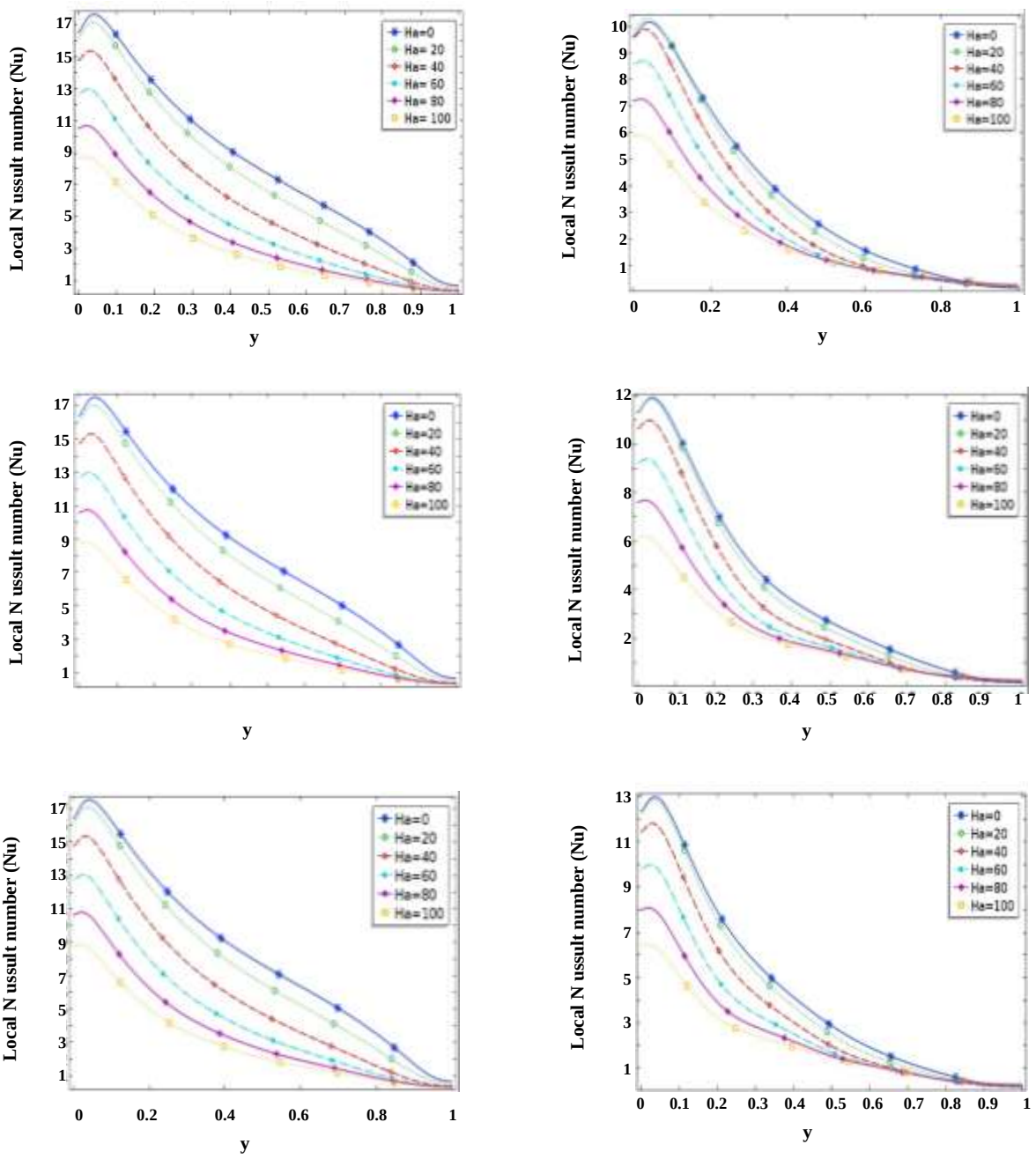

Fig. 13: Local Nussult number along hot wall variation with Ha at φ=0.05 and Ra=10^6. a) Case1. , b) Case2. , and c) Case3.

While the variation of Nusselt number along the hot wall at different Rayleigh and Hartmann numbers is shown in **Fig. 15**. It can be shown from the figure as Darcy number increase from **0.00001 to 0.1** allow to the nanofluid to penetrate through the wavy porous layer due to the enlarged the permeability ***(i.e. transition from conduction to convection heat transfer with the increasing of Darcy number)*** then increase the average Nusselt number. While at a constant Darcy number, the average Nusselt number decreases as the Hartmann number increases for all values of the Rayleigh number due to a decrease in fluid movement and taking a long path to the cold surface which convective heat transfer is restricted in nanofluid layer and became conduction heat transfer

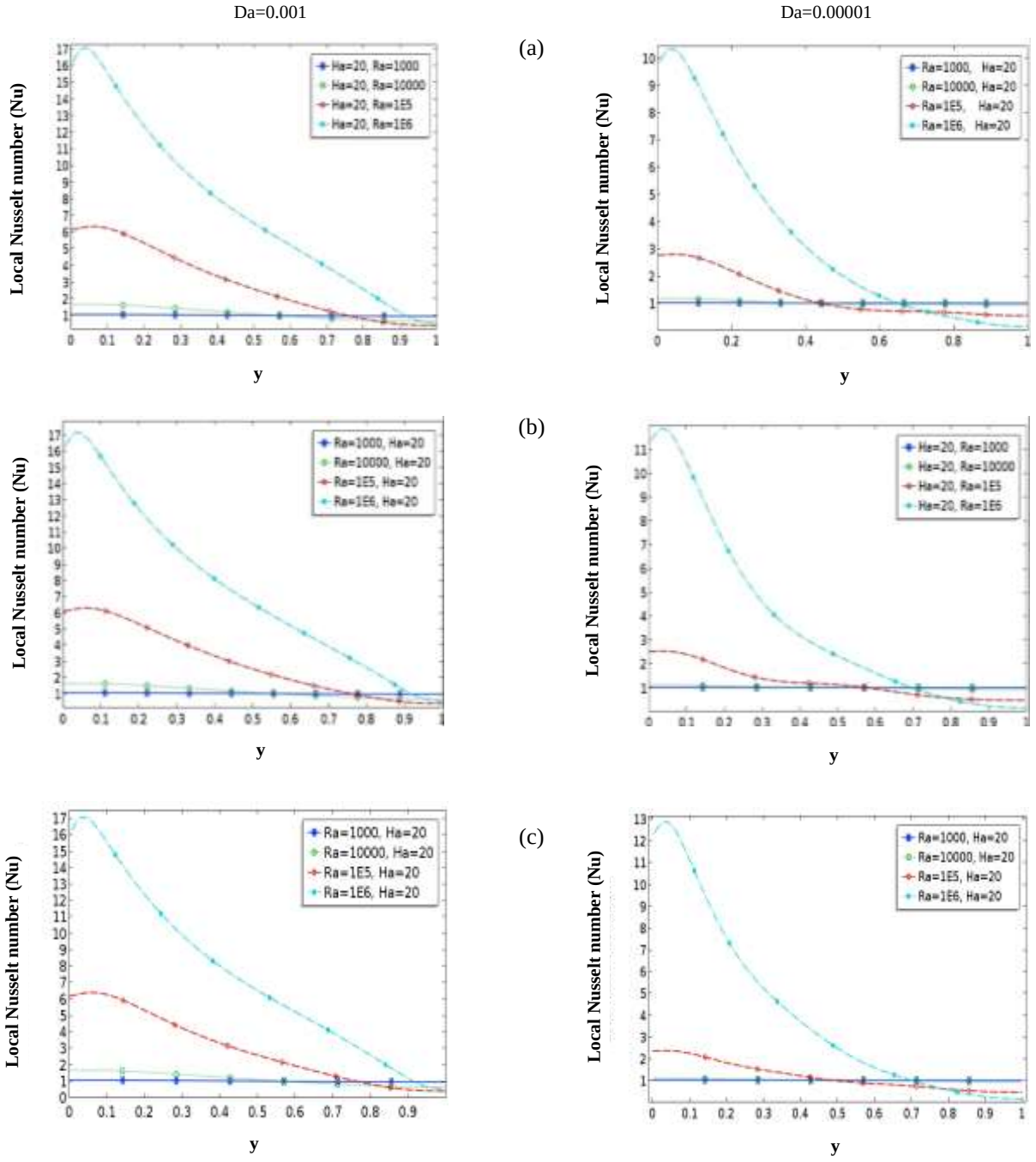

Fig. 14: Local Nussult number along hot wall variation with Ra at φ=0.05 and Ha=20 .a) Case1. , b) Case2. , and c) Case3.

dominates in the wavy porous layer and this is the same reason for reduced the average Nusselt number at a low Darcy number. **Fig. 16** shows the relation between the average Nusselt number and nanoparticles volume fraction for three cases of the wavy porous layer with a different Darcy number. As mentioned above, when the Darcy number increases, the permeability increases and leads to a transition from conduction to convection, so the average Nusselt number increases. While the addition of **TiO_2** nanoparticles has a slight effect on the average Nusselt number that reduced but venially. The effect of nanofluid volume fraction on the average Nusselt number appears at a low Darcy number since the wavy porous layer act as a rigid wall that prevents the nanoparticles

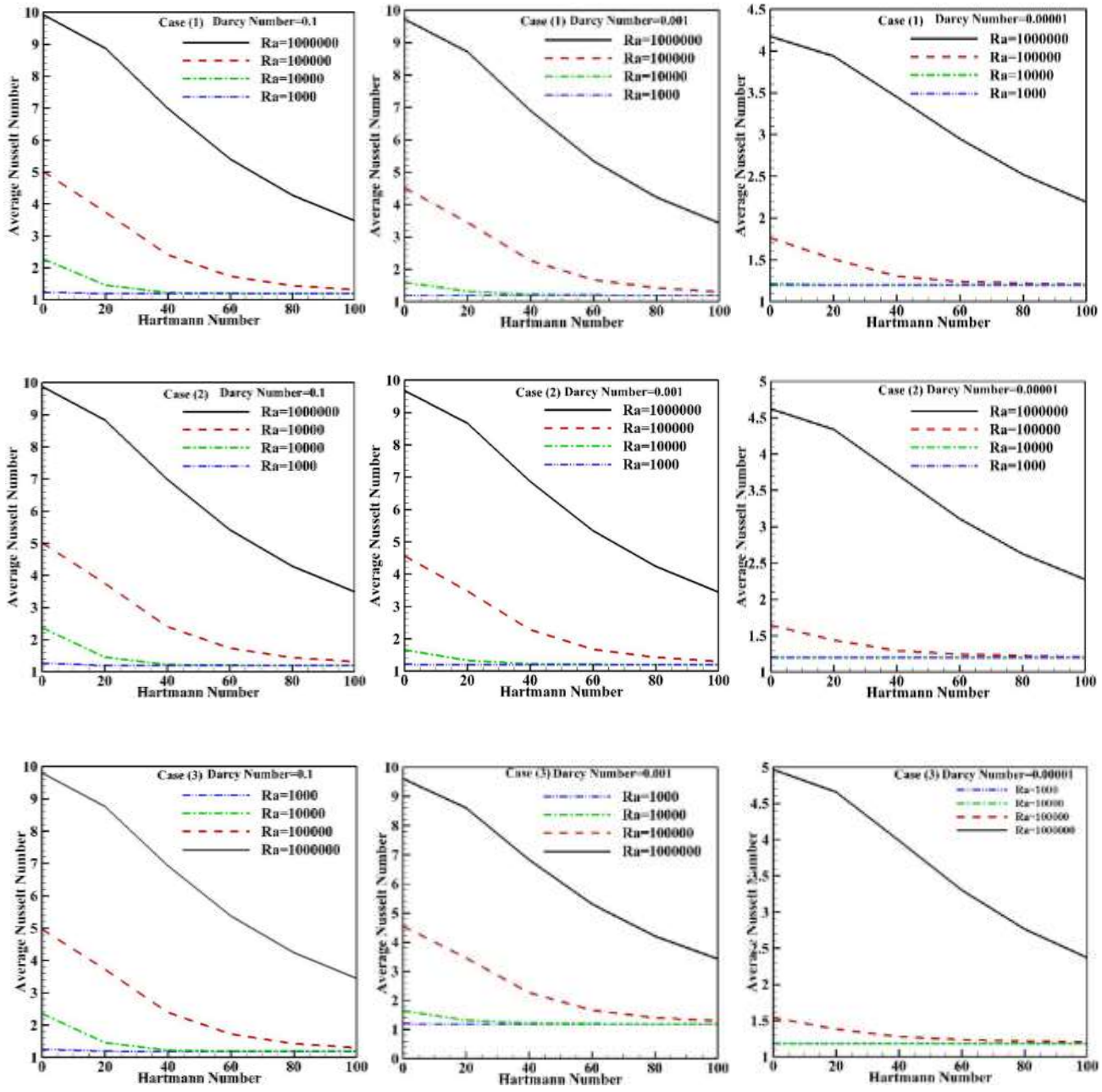

Fig. 15: Average Nussult number along hot wall variation with Hartmann Number for Different Rayleigh Numbers.

from penetrating it. So, the convective heat transfer is restricted on the nanoparticle layer but increased the addition of nanofluid volume fraction enhanced the heat transfer (increase in the wavy porous layer deteriorates the convection heat transfer) in spite of the negative effect due to a low permeability in the nanofluid layers then more drag force.

CONCLUSIONS

The main objective of the current research is the numerical investigation of the heat transfer and fluid flow inside the square enclosure with three cases of the wavy porous layer. The study is performed in the Rayleigh range (10^3-10^6), Darcy number range (10^{-1}-10^{-5}) and nanofluid volume fraction range (0-0.06).

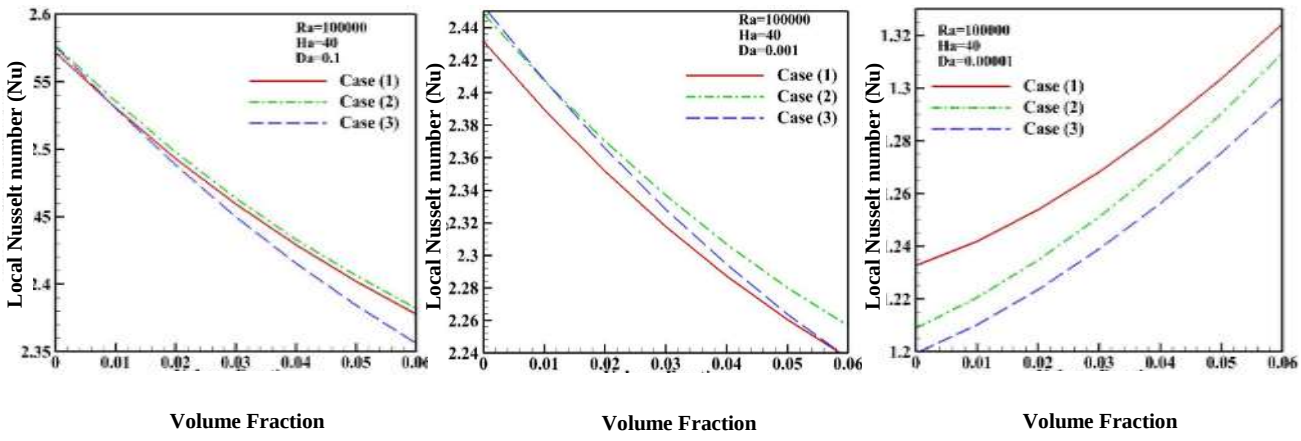

Fig. 16: Average Nussult number along hot wall variation with Volume Fraction for Different Cases.

It can be concluded from the graphical results the following points:

1- The absolute value of the maximum stream function reduces when the Hartmann number increases and decreases of Darcy number for all three cases of the wavy porous layer.

2- Heatlines and Isothermalines increase as the Darcy number is increased.

3- The local Nusselt number decreases as the Hartmann number increases and the Darcy number decreases.

4- The average Nusselt number grows with the rise of the Rayleigh number and drops the Hartmann number.

5- The average Nusselt number reduces as the nanofluid volume fraction increases at a high Darcy number.

Nomenclature

C_p	Specific heat at constant pressure, kJ/kg.K
G	Gravitational acceleration, m/s^2
K	Thermal conductivity, W/m.K
L	Height and Length of the cavity, m
P	Dimensionless pressure
P	Pressure, Pa
Pr	Prandtl number, ν_f/α_f
Ra	Rayleigh number, $g\beta_f L^3 \Delta T/\nu_f \alpha_f$
T	Temperature, K
Ha	Hartmann number
Da	Darcy Number
N	Number of corrugations
Nu_{local}	Local Nusselt number on the hot wall
Nu_{ave}	Average Nusselt number along the hot wall
U	Dimensionless velocity component in x-direction
u	Velocity component in x-direction, m/s
V	Dimensionless velocity component in y-direction
v	Velocity component in y-direction, m/s
X	Dimensionless coordinate in horizontal direction
x	Cartesian coordinates in horizontal direction, m
Y	Dimensionless coordinate in vertical direction
y	Cartesian coordinate in vertical direction, m
n	Normal direction

Greek symbols

A	Thermal diffusivity, m^2/s
Θ	Dimensionless temperature, T-Tc/ΔT
Ψ	Dimensional stream function, m^2/s
Ψ	Dimensionless stream function
M	Dynamic viscosity, kg.s/m
k_{eff}	Effective thermal conductivity
Φ	Volume fraction
Ω	Dimensionless vorticity
Π	Dimensionless heat function
ν	Kinematic viscosity, (μ /ρ)(Pa. s)
c	Nanoparticle volume fraction, %
ω	Vorticity, 1/s
β	Volumetric coefficient of thermal expansion, 1/K
ρ	Density, kg/m^3
ε	Porosity
α_{eff}	Effective thermal diffusivity
σ	Electrical conductivity, W/m.K

Subscripts

C	Cold
Fl	Fluid (pure)
S	Solid

H	Hot
na	Nanofluid
s	Source surface
po	Porous medium

Received : Aug. 10, 2020 ; Accepted : Dec. 27, 2021

REFERENCES

[1] Ali M., Al-Zamily J., Effectiveness and Economic for Using Ag-Nanoparticles in Porous Media Inside Enclosure with Present Heat Generation and Magnetic Field Under Natural Convection Conditions, *Int. J. Fluid Mech. Res.*, **42**: 485–508 (2015).

[2] Ghahremani E., Transient Natural Convection in an Enclosure with Variable Thermal Expansion Coefficient and Nanofluid Properties, *Journal of Applied and Computational Mechanics*, **4(3)**: 133-139 (2018).

[3] Boulahia Z., Wakif A., Sehaqui R., Natural Convection Heat Transfer of the Nanofluids in a Square Enclosure with an Inside Cold Obstacle, *International Journal of Innovation and Scientific Research*, **21(2)**: 367-375 (2016).

[4] Jmai R., Ben-Beya B., Lili T., Heat Transfer and Fluid Flow of Nanofluid-Filled Enclosure with Two Partially Heated Side Walls and Different Nanoparticles, *Superlattices and Microstructures*, **53**: 130-154 (2013).

[5] Khanafer K., Vafai K., Lightstone M., Buoyancy-Driven Heat Transfer Enhancement in a Two-Dimensional Enclosure Utilizing Nanofluids, *International Journal of Heat and Mass Transfer*, **46(19)**: 3639-3653 (2003).

[6] Zhang T., Che D., Double MRT Thermal Lattice Boltzmann Simulation for MHD Natural Convection of Nanofluids in an Inclined Cavity with Four Square Heat Sources, *International Journal of Heat and Mass Transfer*, **94**: 87-100 (2016).

[7] Santra A.K., Sen S., Chakraborty N., Study of Heat Transfer Augmentation in a Differentially Heated Square Cavity Using Copper–Water Nanofluid, *International Journal of Thermal Sciences*, **47(9)**: 1113-1122 (2008).

[8] Muthtamilselvan M., Sureshkumar S., Convective Heat Transfer in a Porous Enclosure Saturated by Nanofluid with Different Heat Sources, *Nonlinear Engineering*, **7(1)**: 1-16 (2018).

[9] Alsabery A., et al., Natural Convection Flow of a Nanofluid in an Inclined Square Enclosure Partially Filled with a Porous Medium, *Scientific Reports*, 7(1): 2357 (2017).

[10] Ismael M.A., Armaghani T., Chamkha A.J., Conjugate Heat Transfer and Entropy Generation in a Cavity Filled with a Nanofluid-Saturated Porous Media and Heated By A Triangular Solid, *Journal of the Taiwan Institute of Chemical Engineers*, **59**: 138-151 (2016).

[11] Alsabery A., et al., Heatline Visualization of Conjugate Natural Convection in a Square Cavity Filled with Nanofluid with Sinusoidal Temperature Variations on Both Horizontal Walls, *International Journal of Heat and Mass Transfer*, **100**: 835-850 (2016).

[12] Badruddin I.A., et al., Conjugate Heat Transfer in an Annulus with Porous Medium Fixed Between Solids, *Transport in Porous Media*, **109(3)**: 589-608 (2015).

[13] Alsabery A., et al., Heatline Visualization of Natural Convection in a Trapezoidal Cavity Partly Filled with Nanofluid Porous Layer and Partly with Non-Newtonian Fluid Layer, *Advanced Powder Technology*, **26(4)**: 1230-1244 (2015).

[14] Selimefendigil F., Öztop H.F., Numerical Study of MHD Mixed Convection in a Nanofluid Filled Lid Driven Square Enclosure with a Rotating Cylinder, *International Journal of Heat and Mass Transfer*, **78**: 741-754 (2014).

[15] Al-Farhany K., Turan A., Unsteady Conjugate Natural Convective Heat Transfer in a Saturated Porous Square Domain Generalized Model, Numerical Heat Transfer, *Part A: Applications*, **60(9)**: 746-765 (2011).

[16] Aminossadati S., Ghasemi B., Natural Convection Cooling of aLocalised Heat Source at the Bottom of a Nanofluid-Filled Enclosure, *European Journal of Mechanics-B/Fluids*, **28(5)**: 630-640 (2009).

[17] Abu-Nada E., Oztop H.F., Effects of Inclination Angle on Natural Convection in Enclosures Filled with Cu–Water Nanofluid, *International Journal of Heat and Fluid Flow*, **30(4)**: 669-678 (2009).

[18] Hussain S.H., Rahomy M.S., Comparison of Natural Convection Around a Circular Cylinder with Different Geometries of Cylinders Inside a Square Enclosure Filled with Ag-Nanofluid Superposed Porous-Nanofluid Layers, *Journal of Heat Transfer*, **141(2)**: 1-29 (2018).

[19] Minh Taun Nguyen, Abdelraheem M. Aly, Sang-Wook Lee, Effect of a Wavy Interface on the Natural Convection of a Nanofluid in a Cavity with a Partially Layered Porous Medium Using the ISPH Method, Numerical Heat Transfer, *Part A: Application*, **72(1)**: 68-88 (2017).

[20] Ali M., Al-Zamily J., Analysis of Natural Convection and Entropy Generation in a Cavity Filled with Multi-Layers of Porous Medium and Nanofluid with a Heat Generation, *International Journal of Heat and Mass Transfer*, **106**: 1218-1231 (2017).

[21] Chamkha A.J., Ismael M.A., Natural Convection in Differentially Heated Partially Porous Layered Cavities Filled with A Nanofluid, *Numerical Heat Transfer, Part A*, **65(11)**: 1089-1113 (2014).

[22] Madera C.G.A., Valdés-Parada F.J., Goyeau B., Tapia J.A.O., Convective Heat Transfer in a Channel Partially Filled with a Porous Medium, *International Journal of Thermal Science*, **50**: 1355-1368 (2011).

[23] Chamkha A.J., Aly A.M., MHD Free Convection Flow of a Nanofluid past a Vertical Plate in the Presence of Heat Generation or Absorption Effects, *Chem. Eng. Comm.*, **198**: 425-441 (2011).

[24] Gobin D., Goyeau B., Neculae A., Convective Heat and Solute Transfer in Partially Porous Cavities, *International Journal of Heat and Mass Transfer*, **48**: 1898–1908 (2005).

[25] Tastsuo Nishimura, Toru Takumi, Mitsuhiro Shiraishi, Yuji Kawamura, Hiroyuki Ozoe, Numerical Analysis of Natural Convection in a Rectangular Enclosure Horizontally Divided into Fluid and Porous Regions, *Int. J. Heat and Mass Transfer*, **29(6)**: 889-898 (1986).

[26] Beckermann C., Ramadhyani S., Viskanta R., Natural Convection Flow and Heat Transfer between a Fluid Layer and a Porous Layer inside a Rectangular Enclosure, *Journal of Heat and Mass Transfer*, **109**: 363-370 (1987).

[27] Hamida M. B., Charrada K., Natural Convection Heat Transfer in an Enclosure Filled with an Ethylene Glycol-Copper Nanofluid under Magnetic Fields, *Numerical Heat Transfer, Part A*, **67(8)**: 902-920 (2014).

[28] Abdulkadhim, Ammar, Hameed K. Hamzah, Farooq H. Ali, Azher M. Abed, Isam Mejbel Abed, Natural Convection Among Inner Corrugated Cylinders Inside Wavy Enclosure Filled With Nanofluid Superposed in Porous–Nanofluid Layers, *International Communications in Heat and Mass Transfer*, **109**: 104350 (2019).

[29] Jafari A., Shahmohammadi A., Mousavi S.M., CFD Investigation of Gravitational Sedimentation Effect on Heat Transfer of a Nano-Ferrofluid, *Iranian Journal of Chemistry and Chemical Engineering (IJCCE)*, **34(1)**: 87-96 (2015).

[30] Mohebbi K., Rafee R., Talebi F., Effects of Rib Shapes on Heat Transfer Characteristics of Turbulent Flow of Al2O3-Water Nanofluid Inside Ribbed Tubes, *Iranian Journal of Chemistry and Chemical Engineering (IJCCE)*, **34(3)**: 61-77 (2015).

[31] Karimdoost Yasuri A., Izadi M., Hatami H., Numerical Study of Natural Convection in a Square Enclosure Filled by Nanofluid with a Baffle in the Presence of Magnetic Field, *Iranian Journal of Chemistry and Chemical Engineering (IJCCE)*, **38(5)**: 209-220 (2019).